

Dynamic collision avoidance for multiple robotic manipulators based on a non-cooperative multi-agent game

Nigora Gafur, Gajanan Kanagalingam and Martin Ruskowski

Abstract—A flexible operation of multiple robotic manipulators in a shared workspace requires an online trajectory planning with static and dynamic collision avoidance. In this work, we propose a real-time capable motion control algorithm, based on non-linear model predictive control, which accounts for static and dynamic collision avoidance. The proposed algorithm is formulated as a non-cooperative game, where each robot is considered as an agent. Each agent optimizes its own motion and accounts for the predicted movement of surrounding agents. We propose a novel approach to formulate the dynamic collision constraints. Additionally, we account for deadlocks that might occur in a setup of multiple robotic manipulators. We validate our algorithm on a pick and place scenario for four collaborative robots operating in a common workspace in the simulation environment Gazebo. The robots are controlled by the Robot Operating System (ROS). We demonstrate, that our approach is real-time capable and, due to the distributed nature of the approach, easily scales to an arbitrary number of robot manipulators in a shared workspace.

Index Terms—Robotic manipulators, collision avoidance, non-cooperative multi-agent game, distributed model predictive control, motion control, deadlock, ROS.

I. INTRODUCTION

Modern industrial processes are increasingly dominated by shorter innovation and product life cycles, reflecting a growing demand for customized products [1]. Consequently, factory systems must become more flexible and adaptable [2], [3]. Robotic manipulators are capable of providing such flexibility due to their complex kinematic chain. Areas of application are, for instance, assembly, disassembly or packaging lines. Operating in a shared workspace, several robotic manipulators can further increase efficiency, minimize the working area and make collaboration possible. Figure 1 constitutes an example of four robotic manipulators sharing the same workspace and performing a pick and place task. Pick and place tasks are commonplace, for example, in disassembly or packaging applications.

Traditionally, the collision-free trajectories of all involved robotic manipulators in industrial applications are computed offline [4]. The reason for this is the deployment of robotic manipulators for repetitive tasks. In case that parts of the production process are changed, a re-planning of collision-free

The authors are with the Chair of Machine Tools and Control Systems, Department of Mechanical and Process Engineering, Technische Universität Kaiserslautern and German Research Center for Artificial Intelligence (DFKI), Kaiserslautern D-67663, Germany (e-mail: nigora.gafur@mv.uni-kl.de)

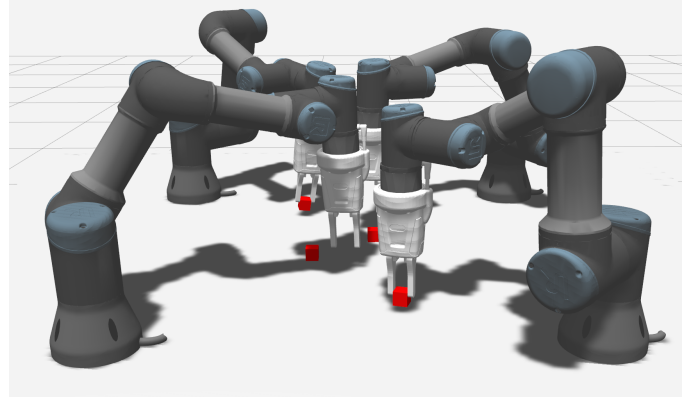


Fig. 1: Setup for a pick and place scenario with four collaborative UR3 manipulators.

trajectories and re-programming of all involved manipulators is necessary. For that reason, it is imperative to develop efficient, scalable and real-time capable motion control strategies which account for static and dynamic obstacles. Such strategies would enable, for example, an on-demand task assignment in a multi-robot setting, giving rise to a more flexible usage of robotic manipulators.

II. RELATED WORK

The problem of motion control is usually split into two sub-problems: *trajectory generation* and *reference tracking control* [5], whereby a collision avoidance strategy is included within one of the former two sub-problems. In industrial applications, the trajectory of manipulators is usually required, in addition to its feasibility, to minimize certain criteria, such as the distance travelled or traveling time, and maximizing others, such as energy efficiency or performance. In addition to that, considering static and dynamic collisions in the environment of the robot is a challenging task.

If the collision avoidance is assigned to *reference tracking control*, the principle of velocity damping [6] can be applied. The method of velocity damping is an established concept in robotics, e.g. applied for self-collision avoidance for humanoid robots [7], [8]. Wang et al. [9] apply the method for a space manipulator with multiple obstacles in the workspace. Obstacles are only considered if the manipulator comes below a predefined distance to these obstacles. Bosscher et al. [10] applies velocity damping for a cooperative motion planning

of two robotic manipulators, where a trajectory is planned for each robot in advance and collisions are considered only during the execution of the trajectory.

Trajectory generation problems are usually formulated as constrained optimization problems [11]. The feasibility of the trajectory is ensured by incorporating a kinematic and a dynamic model of the corresponding manipulator in the constraints of the optimization problem. The concept of model predictive control (MPC) [12] in a "receding horizon" formulation is suitable for solving the *trajectory generation problem*. The framework of MPC, applied for trajectory planning of cooperative and collaborative robotic tasks, allows for the consideration of multiple constraints, i.e. consideration of kinematic as well as static and dynamic collision constraints, into a single optimization problem. The closed-loop control accounts for model uncertainties and disturbances, whereas the predictive nature of MPC gives an insight on the future trajectory. A selection of literature for point-to-point trajectory generation with MPC for a single robotic manipulator without collision avoidance was done by Lam et al. [13], Arkadani et al. [14] and Belda et al. [15].

In general, the motion of a robotic manipulator can either be described in the joint space or the task space. If motion control is described in the task space, a transformation into the joint space (inverse kinematics) is necessary to apply joint torques on the joints' actuators. Inverse kinematics is described by non-linear functions leading to a problem of singularities and non-uniqueness of solutions [16]. Therefore, the proposed methods of collision avoidance applied for other types of robots, such as mobile robots, can not be easily transferred to robotic manipulators.

There are two possible approaches integrating collision avoidance into trajectory generation with MPC. In the first approach, the MPC algorithm itself is extended by solving the optimization problem of MPC not over the whole state space of the considered system, but only over a subset of the state space. This subset excludes all states where a collision might occur and needs to be determined a priori. This method was applied by Liu et al. [17] and Schoels et al. [18] for trajectory generation of a mobile robot, where Schoels et al. [18] approximated the collision free subset by circles and Liu et al. [17] used polyhedra at the current state. Rösmann et al. [19] uses a global planner to optimize trajectories of multiple mobile robots. An extension of these approaches to manipulators is not known to the authors.

The second approach to integrate collision avoidance into trajectory generation with MPC is to introduce further constraints to the optimization problem. There exist several approaches to formulate these constraints. One approach is to restrict the distance of all collision-prone object pairs, where the corresponding objects are approximated by convex bodies. Thus, for a kinematic model of a manipulator this results in a connected chain of convex bodies [10], [20], [21], where each pair of collision-prone bodies introduces an

additional constraint into the optimization problem, e.g., in case of multiple manipulators or manipulator and a human. The computation of distances between two convex bodies is done by algorithms with nested logical conditions [22], [23], [24]. However, the derivatives of the constraints are not smooth, which poses additional challenges to solving the underlying optimization problem. Krämer et al. [21] extends the collision avoidance approach from Lumelsky [22] and proposes an online motion control for one robotic manipulator in a collaboration with a human. The computation times prove the efficacy of the approach, where the optimization problem is solved with a self developed hypergraph [25] to mitigate the problem of nested logical conditions. Cascio et al. [20] formulates a smooth optimal control problem for two simple two-link manipulators and treats the distance computation by minimizing additional sub-problems with inequality constraints. Each potential collision needs a set of Lagrange multipliers. However, the computation times are not mentioned by the authors.

As an alternative to restricting the distance, virtual hyperplanes can be used to separate two collision-prone bodies. By approximating the considered objects by polyhedra and applying Farkas' lemma, collisions of the considered objects can be avoided. An implementation with multidimensional polyhedra was proposed by Gerdts et al. for a robotic manipulator [26]. In the work of Zhang et al. [27] this approach is extended so that, in addition to collision avoidance, a minimum distance between two bodies can be guaranteed. The former approach comes with the disadvantage, that for every pair of collision-prone objects, several constraints have to be added to the underlying optimization problem. Six new optimization variables have to be introduced into the optimization problem for each considered object pair. The number of additional constraints depends linearly on the number of polyhedron faces.

The framework of MPC can be realized in a centralized or distributed fashion. The drawback of the centralized MPC is the limited scalability and high computational complexity [28]. A distributed MPC framework in the context of game theory can help to split the computational burden, where each agent optimizes its own objective function [28]. This concept was already introduced for robot-human collaboration by Flad et al. [29]. Yanhao et al. [30] proposes an approach based on a distributed control for a cooperative manipulation of an object. Tika et al. applied centralized MPC [31] and distributed MPC [32] for a synchronous pick and place scenario for two robotic manipulators. However, the focus lies on a synchronous task accomplishment for two robotic manipulators rather than collision avoidance. Furthermore, deadlocks are not treated in any of the mentioned works. Existing approaches, still, cannot guarantee a collision-free trajectory generation, that are real-time capable and scale to more than two manipulators.

III. CONTRIBUTION AND OUTLINE

This article is concerned with developing an online motion control algorithm which enables several manipulators

to operate simultaneously in a common workspace. We formulate the problem of online motion control for each manipulator as an optimization problem in the joint space, which incorporates static and dynamic collision avoidance into the trajectory generation problem. To this end, we derive a novel approach for dynamic collision avoidance. Our approach is based on MPC to account for disturbances and uncertainties during motion control. We take special care to ensure that our approach is real-time capable. To this end, we use the concept of distributed MPC in the joint space, based on non-cooperative games, where each robotic manipulator is considered as an agent and shares the predicted trajectory with its neighbours. Furthermore, we introduce a concept how deadlocks among two or more robotic manipulators can be detected and, subsequently, be resolved.

To demonstrate the efficiency of our approach, we consider a setup of four 6-degrees of freedom robotic manipulators (see Figure 1) in the simulation environment *Gazebo* [33], and controlled by the Robot Operating System (ROS) [34], as a benchmark problem. The robotic manipulators are closely placed to each other to operate in a common workspace. We assign each robot a task of picking an object and bringing it back to the robot's initial position. The four objects are placed such that a deadlock is imminent between three of the four robots. We show that such deadlocks are detected and resolved reliably. Furthermore, we demonstrate that our approach efficiently resolves robot-robot collisions in real-time.

The remainder of this article is organized as follows. In Section IV the dynamic model of a robotic manipulator will be introduced, followed by a formulation of the MPC problem in Section V. A novel approach for collision avoidance will be explained in detail in Section VI. Further, deadlock detection and resolution will be discussed in Section VII. Validation of our algorithm and simulation results will be shown in Section VIII followed by a conclusion in Section IX.

IV. DYNAMIC MODEL

We consider a robotic manipulator with N joints and neglect viscous and static friction. The dynamic model of the manipulator can be derived by means of the Lagrangian formalism and written in a matrix form as

$$\mathbf{M}(\mathbf{q}(t))\ddot{\mathbf{q}}(t) + \mathbf{C}(\mathbf{q}(t), \dot{\mathbf{q}}(t))\dot{\mathbf{q}}(t) + \mathbf{g}(\mathbf{q}(t)) = \boldsymbol{\tau}(t), \quad (1)$$

where $\mathbf{q}(t) \in \mathbb{R}^N$ denotes the vector of generalized coordinates, which is the joint angular position vector. Furthermore, $\mathbf{M}(\mathbf{q}(t)) \in \mathbb{R}^{N \times N}$ represents the inertia matrix, $\mathbf{C}(\mathbf{q}(t), \dot{\mathbf{q}}(t)) \in \mathbb{R}^{N \times N}$ maps the angular velocities $\dot{\mathbf{q}}(t)$ to Coriolis and centrifugal torques, $\mathbf{g}(\mathbf{q}(t)) \in \mathbb{R}^N$ is the vector of gravitational and $\boldsymbol{\tau} \in \mathbb{R}^N$ denotes the vector of generalized torques.

Choosing the generalized torques as a state feedback in the form

$$\boldsymbol{\tau}(t) = \mathbf{M}(\mathbf{q}(t))\mathbf{u}(t) + \mathbf{C}(\mathbf{q}(t), \dot{\mathbf{q}}(t))\dot{\mathbf{q}}(t) + \mathbf{g}(\mathbf{q}(t)), \quad (2)$$

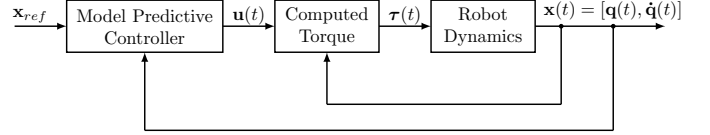


Fig. 2: Control structure with model predictive controller as a top level controller and computed torque controller as a low level controller for generating joint actuator torques.

and assuming that $\mathbf{M}(\mathbf{q}(t))$ is invertible, the non-linear dynamics of a robotic manipulator can be compensated yielding

$$\ddot{\mathbf{q}}(t) = \mathbf{u}(t). \quad (3)$$

The new input $\mathbf{u}(t) \in \mathbb{R}^N$ compensates the non-linearity of the system dynamics given in (1). The non-linear control law in (2), referred to as inverse dynamics control or computed torque, leads to N double integrators for a closed loop system. The control structure of a robotic manipulator is shown in Figure 2. The robot model reduces to

$$\begin{bmatrix} \dot{\mathbf{q}}(t) \\ \ddot{\mathbf{q}}(t) \end{bmatrix} = \begin{bmatrix} \mathbf{0} & \mathbf{I} \\ \mathbf{0} & \mathbf{0} \end{bmatrix} \begin{bmatrix} \mathbf{q}(t) \\ \dot{\mathbf{q}}(t) \end{bmatrix} + \begin{bmatrix} \mathbf{0} \\ \mathbf{I} \end{bmatrix} \mathbf{u}(t), \quad (4)$$

where each joint of a manipulator is independently influenced by the control input. The matrix $\mathbf{I} \in \mathbb{R}^{N \times N}$ denotes the identity matrix and $\mathbf{0} \in \mathbb{R}^{N \times N}$ the zero matrix. In state-space representation, the former reformulates to

$$\dot{\mathbf{x}}(t) = \mathbf{A}\mathbf{x}(t) + \mathbf{B}\mathbf{u}(t) \quad (5)$$

with the state vector $\mathbf{x}(t) = [\mathbf{q}(t)^T \ \dot{\mathbf{q}}(t)^T]^T \in \mathbb{R}^{2N}$, the state matrix $\mathbf{A} \in \mathbb{R}^{2N \times 2N}$ and the input matrix $\mathbf{B} \in \mathbb{R}^{2N \times N}$ [16]. The linear system in (4) describes the dynamics of a robotic manipulator in the joint space, which will be integrated as a constraint together with static and dynamic collision avoidance constraints into an optimization problem. This will be discussed in more detail in Sections V and VI.

V. DISTRIBUTED MODEL PREDICTIVE CONTROL IN THE CONTEXT OF GAME THEORY

We consider a system of M robotic manipulators. Each manipulator $i = 1, \dots, M$ represents an independent subsystem. The main objective of performing a cooperative task is, for every robotic manipulator, to safely reach the target joint state accounting for static, dynamic and self-collision constraints.

Centralized MPC considers the overall system dynamics in a single optimization problem with respect to a common objective function, which can be written as

$$u_1^*, \dots, u_M^* = \arg \min_{u_1, \dots, u_M} J(u_1, \dots, u_M), \quad (6)$$

where u_1^*, \dots, u_M^* are the optimal control inputs of M robotic manipulators.

In this work, we investigate distributed model predictive control (DMPC), where each robot is considered as an agent. There is a multitude of different architectures for distributed

model predictive control [28]. From the point of view of game theory and by classification via the cost function, DMPC can be realized as a cooperative or a non-cooperative game. Both games rely upon communication between the agents.

In a cooperative game, all agents optimize a *global* cost function J , i.e. the agents share a common objective. Cooperative agents negotiate until they agree upon a strategy that brings the best benefit to all of them. For instance, a cooperative game involving M agents, M optimization problems of the form

$$\begin{aligned} u_1^* &= \arg \min_{u_1} J(u_1, u_2^*, \dots, u_{M-1}^*, u_M^*), \\ &\vdots \\ u_M^* &= \arg \min_{u_M} J(u_1^*, u_2^*, \dots, u_{M-1}^*, u_M) \end{aligned} \quad (7)$$

have to be solved.

In a non-cooperative setting, the agents pursue their own goal and therefore act egoistically to achieve their own best possible benefit. Each agent optimizes its own, i.e. *local* cost function J_i , $i = 1, \dots, M$. The non-cooperative game has the following form

$$\begin{aligned} u_1^* &= \arg \min_{u_1} J_1(u_1, u_2^*, \dots, u_{M-1}^*, u_M^*), \\ &\vdots \\ u_M^* &= \arg \min_{u_M} J_M(u_1^*, u_2^*, \dots, u_{M-1}^*, u_M). \end{aligned} \quad (8)$$

The non-cooperative game converges towards a Nash equilibrium [28], whereas the optimal solution of a cooperative game is Pareto optimal [35].

In general, systems considered in a cooperative (7) and a non-cooperative framework (8) are coupled in control inputs, such that each subsystem can not be optimized independently without knowledge of the optimal strategies of other agents. Considering robotic manipulators, the system dynamics are decoupled in states and control inputs. A coupling of the robots' system dynamics occurs e.g., if robotic manipulators are physically attached to each other, which is not the case in this work.

Incorporating collision avoidance constraints leads to a coupling in states for M robotic manipulators. The local cost functions J_i of each agent still remain decoupled in states and control inputs with regard to other agents. The drawback of cooperative DMPC is that each *local* controller has to have knowledge of the full system dynamics and several communication iterations are needed until an optimal solution for the whole game is obtained. Therefore, we consider a non-cooperative game in the following, which has the benefit of local subsystems and local cost functions as well as single communication iteration at each time step.

Keeping the former in mind, we turn our attention to the formulation of the online trajectory planning problem based on

DMPC, formulated as a non-cooperative game. We formalize the proposed motion planning algorithm in the joint space as a finite-horizon continuous-time optimal control problem (OCP). The OCP of manipulator i takes the following form

$$\min_{\mathbf{u}_i(t)} J_i^f(\mathbf{x}_i(t_f)) + \int_{t_0}^{t_f} J_i^c(\mathbf{x}_i(t), \mathbf{u}_i(t)) dt \quad (9)$$

$$s.t. \quad \dot{\mathbf{x}}_i(t) = \mathbf{A}_i \mathbf{x}_i(t) + \mathbf{B}_i \mathbf{u}_i(t), \quad (9a)$$

$$\mathbf{x}_i(t_0) = \mathbf{x}_i^s, \quad (9b)$$

$$\mathbf{x}_i(t) \in \bar{\mathbb{X}}_i, \quad (9c)$$

$$\mathbf{u}_i(t) \in \bar{\mathbb{U}}_i, \quad (9d)$$

$$R_i(\mathbf{x}_i(t)) \cap \mathcal{O} = \emptyset, \quad (9e)$$

$$R_i(\mathbf{x}_i(t)) \cap \mathcal{R}_{-i}(\underline{\mathbf{x}}_i^*(t)) = \emptyset. \quad (9f)$$

The quadratic cost function $J_i^c : \mathbb{R}^{2N} \times \mathbb{R}^N \rightarrow \mathbb{R}$,

$$\begin{aligned} J_i^c(\mathbf{x}_i(t), \mathbf{u}_i(t)) := & (\mathbf{x}_i(t) - \mathbf{x}_i^f)^T \mathbf{Q}_i^x (\mathbf{x}_i(t) - \mathbf{x}_i^f) + \\ & \mathbf{u}_i(t)^T \mathbf{R}_i^u \mathbf{u}_i(t) + \dot{\mathbf{u}}_i(t)^T \mathbf{R}_i^d \dot{\mathbf{u}}_i(t) \end{aligned} \quad (10)$$

penalizes the squared state error, i.e., the deviation of the state $\mathbf{x}_i(t)$ from the desired state $\mathbf{x}_i^f = [\mathbf{q}_i^{f \top} \mathbf{0}^T]^T$, the magnitude of the control input $\mathbf{u}_i(t)$ and the control smoothness, i.e., the magnitude of $\dot{\mathbf{u}}_i(t)$, with the positive (semi-) definite weighting matrices $\mathbf{Q}_i^x \in \mathbb{R}^{2N \times 2N}$, $\mathbf{R}_i^u \in \mathbb{R}^{N \times N}$ and $\mathbf{R}_i^d \in \mathbb{R}^{N \times N}$, respectively. The terminal state cost $J_i^f : \mathbb{R}^{2N} \rightarrow \mathbb{R}$

$$J_i^f(\mathbf{x}_i(t_f)) := (\mathbf{x}_i(t_f) - \mathbf{x}_i^f)^T \mathbf{Q}_i^f (\mathbf{x}_i(t_f) - \mathbf{x}_i^f) \quad (11)$$

penalizes the terminal squared state error with the positive (semi-) definite weighting matrix $\mathbf{Q}_i^f \in \mathbb{R}^{2N \times 2N}$.

The dynamics of manipulator i is given by equation (9a), see Section IV, whereas the equation (9b) sets the measured joint state \mathbf{x}_i^s of manipulator i as the initial condition of the state vector $\mathbf{x}_i(t)$ at time $t = t_0$. The equations (9c) and (9d) represent lower and upper bounds on the states and control inputs, i.e.,

$$\begin{aligned} \bar{\mathbb{X}}_i &:= \{\mathbf{x}_i(t) \in \mathbb{R}^{2N} \mid \mathbf{x}_{i,\min} \leq \mathbf{x}_i(t) \leq \mathbf{x}_{i,\max}\}, \\ \bar{\mathbb{U}}_i &:= \{\mathbf{u}_i(t) \in \mathbb{R}^N \mid \mathbf{u}_{i,\min} \leq \mathbf{u}_i(t) \leq \mathbf{u}_{i,\max}\}. \end{aligned} \quad (12)$$

The equation for joint angles (12) also accounts for self-collision constraints through limitation of the joints' angle ranges.

We formulate static and dynamic collision avoidance constraints in the task space, transforming joint positions into positions in Cartesian space using the non-linear forward kinematics. The collision avoidance constraints turn the optimization problem (9) into a non-linear distributed OCP. We define the set

$$\mathcal{R}(\underline{\mathbf{x}}(t)) := R_1(\mathbf{x}_1(t)) \cup \dots \cup R_M(\mathbf{x}_M(t)), \quad (13)$$

where $R_i(\mathbf{x}_i(t))$ denotes the interior set of Cartesian points occupied by manipulator i with state $\mathbf{x}_i(t)$. The trajectory vector $\underline{\mathbf{x}}(t) = [\mathbf{x}_1(t), \dots, \mathbf{x}_M(t)]$ collects the trajectories of all involved robots. To account for static objects in the task space, we define the set \mathcal{O} containing all interior points of all static obstacles. Indeed, constraint (9e) enforces that the intersection of $R_i(\mathbf{x}_i(t))$ and the obstacles \mathcal{O} for state $\mathbf{x}_i(t)$ is empty.

To consider dynamic collision avoidance constraints, i.e., the prevention of inter-robot collisions, the short-hand notation

$$\mathcal{R}_{-i}(\underline{\mathbf{x}}_{-i}(t)) := \mathcal{R}(\underline{\mathbf{x}}(t)) \setminus R_i(\mathbf{x}_i(t)) \quad (14)$$

with

$$\underline{\mathbf{x}}_{-i}(t) = [\mathbf{x}_1(t), \dots, \mathbf{x}_{i-1}(t), \mathbf{x}_{i+1}(t), \dots, \mathbf{x}_M(t)] \quad (15)$$

is introduced. Consequently, constraint (9f) prevents the inter-robot collision of robot i with all other robots. The efficient implementation of constraints (9e) and (9f) is the topic of the following section. In the following, we focus on solving the DMPC before turning to the efficient implementation of the collision avoidance constraints.

Note, that constraint (9f) establishes the coupling between the manipulators. Constraint (9f) implies that the optimal trajectories of all other robots, collected in $\underline{\mathbf{x}}_{-i}^*(t)$, is known a priori in order to solve the OCP for manipulator i . Due to the couplings between the manipulators solving the continuous-time OCP (9) is challenging. In order to solve the M OCPs and determine the optimal control inputs of all robots efficiently, the continuous-time optimal control problem needs to be discretized first.

We choose the multiple shooting method for discretizing problem (9). The prediction horizon $t \in [t_0, t_f]$ is split equidistantly into N_p uniform time steps at times $t_k = t_0 + k \cdot T_s$ for $k = 0, \dots, N_p$ and a sample time T_s . The discrete states are denoted in the following as $\mathbf{x}_i^k = \mathbf{x}_i(t_k)$ and discrete control inputs as $\mathbf{u}_i^k = \mathbf{u}_i(t_k)$. With the short-hand notation for the states $\mathbf{x}_i^{0:N_p} = [\mathbf{x}_i^0, \dots, \mathbf{x}_i^{N_p}]$ and the control inputs $\mathbf{u}_i^{0:N_p-1} = [\mathbf{u}_i^0, \dots, \mathbf{u}_i^{N_p-1}]$, the problem takes the following form

$$\min_{\mathbf{u}_i^{0:N_p-1}, \mathbf{x}_i^{0:N_p}} J_i^f(\mathbf{x}_i^{N_p}) + \sum_{k=0}^{N_p-1} J_i^c(\mathbf{x}_i^k, \mathbf{u}_i^k) \quad (16)$$

$$s.t. \quad \mathbf{x}_i^{k+1} = \mathbf{A}_i^d \mathbf{x}_i^k + \mathbf{B}_i^d \mathbf{u}_i^k, \quad k = 0, \dots, N_p - 1, \quad (16a)$$

$$\mathbf{x}_i^0 = \mathbf{x}_i^s, \quad (16b)$$

$$\mathbf{x}_i^k \in \bar{\mathbb{X}}_i, \quad k = 0, \dots, N_p, \quad (16c)$$

$$\mathbf{u}_i^k \in \bar{\mathbb{U}}_i, \quad k = 0, \dots, N_p, \quad (16d)$$

$$R_i(\mathbf{x}_i^k) \cap \mathcal{O} = \emptyset, \quad k = 0, \dots, N_p, \quad (16e)$$

$$R_i(\mathbf{x}_i^k) \cap \mathcal{R}_{-i}(\underline{\mathbf{x}}_{-i}^k) = \emptyset, \quad k = 0, \dots, N_p. \quad (16f)$$

Here, the matrices \mathbf{A}_i^d and \mathbf{B}_i^d are discrete representations of state and input matrices of manipulator i .

To obtain

$$\underline{\mathbf{x}}_{-i}^{*0:N_p} = [\underline{\mathbf{x}}_1^{*0:N_p}, \dots, \underline{\mathbf{x}}_{i-1}^{*0:N_p}, \underline{\mathbf{x}}_{i+1}^{*0:N_p}, \dots, \underline{\mathbf{x}}_M^{*0:N_p}], \quad (17)$$

for collision constraint (16f) of each manipulator $i = 1, \dots, M$ we use an extrapolation approach [28]. Suppose

$$\underline{\mathbf{x}}_{-i}^{*0:N_p} = [\hat{\mathbf{x}}_1^{*0:N_p}, \dots, \hat{\mathbf{x}}_M^{*0:N_p}] \quad (18)$$

denotes the manipulators' optimal trajectories from the last converged DMPC-step. We obtain $\underline{\mathbf{x}}_i^{*0:N_p}$ (and thus also $\underline{\mathbf{x}}_{-i}^{*0:N_p}$) by shifting $\hat{\mathbf{x}}_{-i}^{*0:N_p}$ by one time step and extrapolating the last state. In other words, for every manipulator $i = 1, \dots, M$, we compute

$$\mathbf{x}_i^{*0:N_p} = [\hat{\mathbf{x}}_i^{*1:N_p} \quad \mathbf{x}_i^{*N_p}]. \quad (19)$$

where the last predicted optimal state $\mathbf{x}_i^{*N_p}$ is obtained by the extrapolation of $\hat{\mathbf{x}}_i^{*N_p}$ using the discrete system dynamics, i.e.,

$$\mathbf{x}_i^{*N_p} = \mathbf{A}_i^d \hat{\mathbf{x}}_i^{*N_p} + \mathbf{B}_i^d \mathbf{u}_i^{*N_p-1}. \quad (20)$$

Note, that the equation (20) can be obtained by setting $\mathbf{u}_i^{*N_p-1} = \hat{\mathbf{u}}_i^{*N_p-1}$, i.e. the two last optimal inputs in the sequence $\mathbf{u}_i^{*0:N_p-1}$ are equal.

To sum up, the model predictive controller of each robot receives its current joint state and the (extrapolated) predicted joint states of neighboured robots denoted as

$$\underline{\mathbf{x}}_{-i}^{*0:N_p} = [\underline{\mathbf{x}}_1^{*0:N_p}, \dots, \underline{\mathbf{x}}_{i-1}^{*0:N_p}, \underline{\mathbf{x}}_{i+1}^{*0:N_p}, \dots, \underline{\mathbf{x}}_M^{*0:N_p}] \quad (21)$$

to account for collisions in the future and choose a proper control strategy to avoid them.

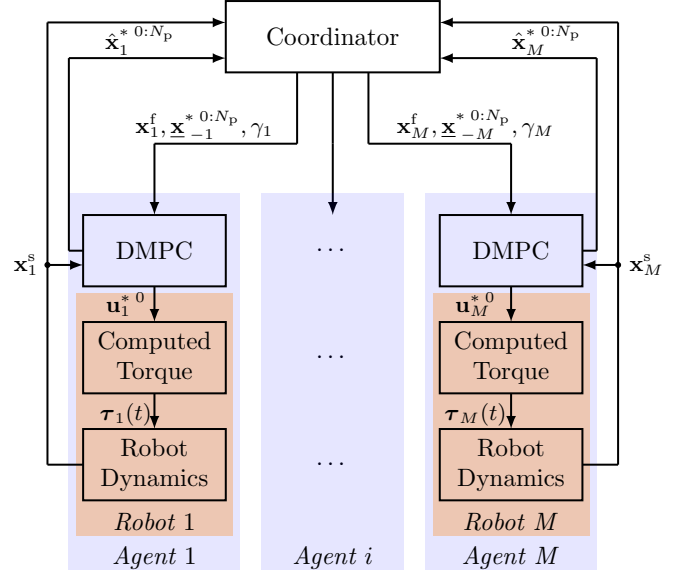


Fig. 3: Control structure of collision free online motion control for multiple robotic manipulators.

The control structure of our approach is illustrated in Figure 3. The supervisory role is taken by a coordinator, that receives all predicted state sequences $\hat{\mathbf{x}}_i^{*0:N_p}$ for $i = 1, \dots, M$ of the last converged DMPC step. The coordinator detects whether a deadlock is present and resolves it with a decision parameter γ_i . This will be discussed in more detail in Section VII. The coordinator has knowledge about the system dynamics of each agent and extrapolates $\hat{\mathbf{x}}_i^{*0:N_p}$ for $i = 1, \dots, M$ as previously explained and sends the extrapolated predicted state sequences $\underline{\mathbf{x}}_{-i}^{*0:N_p}$, $i = 1, \dots, M$ to all robots. To increase the efficiency, the warm starts of the solver are initialized with the previously obtained optimal solutions in states and control inputs. The

model predictive controllers of the M agents solve the problem (16) in parallel. The optimal control inputs $\mathbf{u}_i^{*0} = \text{const.}$, $i = 1, \dots, M$ for $[t_0, t_1]$ are sent to the robots' underlying computed torque controllers. The computed torque controller generates joint actuator torques $\tau_i(t)$ which are applied to each robots' joints. At the same time, the obtained optimal state sequence $\hat{\mathbf{x}}_i^{0:N_p}$, $i = 1, \dots, M$ is sent to the coordinator. Subsequently, the current state of a robot \mathbf{x}_i^s , $i = 1, \dots, M$ is sent to the DMPC.

VI. COLLISION AVOIDANCE METHOD FOR MULTIPLE ROBOTIC MANIPULATORS

In the previous section, we formulated the motion control problem of M robotic manipulators as M coupled DMPCs, based on non-cooperative games. This section is dedicated to the efficient implementation of the static and dynamic collision constraints (16e) and (16f).

One of the most applied algorithms among collision avoidance methods in the literature is the Lumelsky algorithm [22]. The method approximates the robot links with line segments and introduces an algorithm to compute the minimum distance between two line segments. The approximation of robot links as line segments is also known as line-swept sphere [10], [21], [20]. The drawback of the algorithm are the nested logical conditions, which are not smooth and pose challenges to solving the OCP. Therefore, we introduce a novel approach for collision avoidance by approximating a robot's geometry by line segments and ellipsoids and derive an efficient and smooth formulation, that enables the robots to safely avoid collisions.

A. Ellipsoid - line segment approach

In order to overcome the problem with nested logical conditions, we do not use a distance function to compute the distance between two links. Instead we check if a line segment intersects with an ellipsoid. In the following, we proceed from the perspective of a manipulator i with a set of interior points in the task space denoted by $R_i(\mathbf{x}_i^k)$. The sets of interior points of the other robotic manipulators is designated by $\mathcal{R}_{-i}(\underline{\mathbf{x}}_{-i}^k)$. We approximate the links of a manipulator i , for which the optimization problem is solved, by line segments and the links of the remaining manipulators by ellipsoids. See Figure 4 for an illustration. By ensuring that the ellipsoids are sufficiently large and the lines and ellipsoids do not intersect, we assure that

$$R_i(\mathbf{x}_i^k) \cap \mathcal{R}_{-i}(\underline{\mathbf{x}}_{-i}^k) = \emptyset, \quad k = 0, \dots, N_p \quad (22)$$

holds. Please note, that all pairs of ellipsoids and line segments of all involved robotic manipulators must be taken into account for every time step $k = 0, \dots, N_p$.

In the following we consider collision avoidance between a robot i and a robot j , where robot i is modeled with line segments and robot j with ellipsoids. A line segment \mathbf{s}_m of a link m is described by the equation

$$\mathbf{s}_m(\mathbf{x}_i^k) := \mathbf{b}_m(\mathbf{x}_i^k) + \alpha_m \mathbf{r}_m(\mathbf{x}_i^k), \quad \alpha_m \in [0, 1], \quad (23)$$

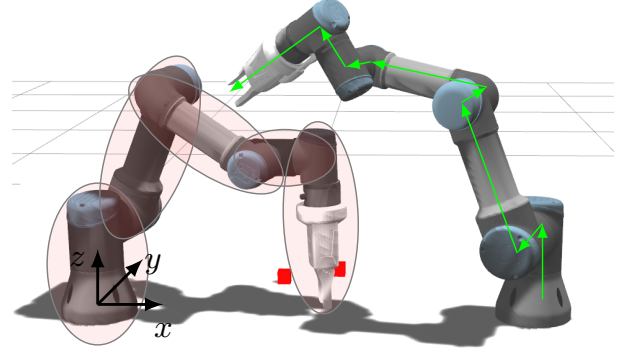


Fig. 4: Illustrative approximation of robots' geometry with ellipsoids and line segments from the perspective of the robot $R_i(\cdot)$ on the right side.

where vector $\mathbf{b}_m(\mathbf{x}_i^k) \in \mathbb{R}^3$ is the position vector of the basis of the considered link and vector $\mathbf{r}_m(\mathbf{x}_i^k) \in \mathbb{R}^3$ designates the direction from $\mathbf{b}_m(\mathbf{x}_i^k)$ to $\mathbf{b}_{m+1}(\mathbf{x}_i^k)$ of the subsequent link. The parameter α_m restricts the line segment to the length of the considered link.

The ellipsoid $\{\mathbf{x}_j^k \in \mathbb{R}^{2N} \mid H_n(\mathbf{e}, \mathbf{x}_j^k) = 1\}$ of a link n is given by the following quadratic equation

$$H_n(\mathbf{e}, \mathbf{x}_j^k) := (\mathbf{e} - \mathbf{e}_{0,n}(\mathbf{x}_j^k))^T \mathbf{R}_n(\mathbf{x}_j^k) \mathbf{E}_n \mathbf{R}_n^T(\mathbf{x}_j^k) (\mathbf{e} - \mathbf{e}_{0,n}(\mathbf{x}_j^k)), \quad (24)$$

where $\mathbf{e} \in \mathbb{R}^3$ names a point on the ellipsoid. The centre point of the ellipsoid is denoted

$$\mathbf{e}_{0,n}(\mathbf{x}_j^k) = \frac{1}{2}(\mathbf{b}_{n+1}(\mathbf{x}_j^k) + \mathbf{b}_n(\mathbf{x}_j^k)), \quad (25)$$

the rotation matrix $\mathbf{R}_n(\mathbf{x}_j^k) \in \text{SO}(3)$ describes the rotation of link n relative to the inertial frame of reference and the diagonal matrix

$$\mathbf{E}_n = \text{diag} \left(\frac{1}{l_1^2}, \frac{1}{l_2^2}, \frac{1}{l_3^2} \right) \in \mathbb{R}^{3 \times 3} \quad (26)$$

contains the squared inverse principal semi-axes $l_1, l_2, l_3 \in \mathbb{R}_{>0}$. To ensure that (22) holds, the width of an ellipsoid should be at least twice as large as the width of a robot link and the ellipsoid should also occupy the two joints connecting the link.

In order to ensure, that line segment m and ellipsoid n do not intersect, the condition

$$1 - H_n(\mathbf{s}_m(\mathbf{x}_i^k), \mathbf{x}_j^k) \leq 0, \quad \forall \alpha_m \in [0, 1] \quad (27)$$

has to hold. Alternatively, the former can be reformulated into an optimization problem, i.e., solving

$$\min_{\alpha_m} H_n(\mathbf{b}_m + \alpha_m \mathbf{r}_m) \quad (28)$$

$$\text{s.t. } 0 \leq \alpha_m \leq 1 \quad (28a)$$

for α_m^* where $H_n(\mathbf{b}_m + \alpha_m^* \mathbf{r}_m) \geq 1$ holds. Please note, we dropped explicit reference to \mathbf{x}_i^k and \mathbf{x}_j^k for sake of readability. Problem (28) is solved in the following way. First, the solution

$\hat{\alpha}_m \in [-\infty, \infty]$ of the unconstrained optimization problem computes to

$$\hat{\alpha}_m = -\frac{(\mathbf{b}_m - \mathbf{e}_{0,n})^T \mathbf{R}_n \mathbf{E}_n \mathbf{R}_n^T \mathbf{r}_m}{\mathbf{r}_m^T \mathbf{R}_n \mathbf{E}_n \mathbf{R}_n^T \mathbf{r}_m}. \quad (29)$$

The former is guaranteed to exist since $H_n(\mathbf{e})$ is positive definite, i.e., $\mathbf{r}_m^T \mathbf{R}_n \mathbf{E}_n \mathbf{R}_n^T \mathbf{r}_m > 0$ holds. Projecting $\hat{\alpha}_m$ onto the unit interval by the projection operator $P : (-\infty, \infty) \rightarrow [0, 1]$ gives rise to the solution α_m^* of (28) in closed form

$$\alpha_m^* = P\left(-\frac{(\mathbf{b}_m - \mathbf{e}_{0,n})^T \mathbf{R}_n \mathbf{E}_n \mathbf{R}_n^T \mathbf{r}_m}{\mathbf{r}_m^T \mathbf{R}_n \mathbf{E}_n \mathbf{R}_n^T \mathbf{r}_m}\right). \quad (30)$$

Since P is not continuously differentiable, we approximate P by

$$\hat{P}(\alpha) = \alpha \Phi(\alpha) - (\alpha - 1) \Phi(\alpha - 1) \quad (31)$$

where Φ refers to the smooth approximation of the Heaviside function

$$\Phi(\alpha) = \frac{1}{1 + \exp(-c\alpha)} \quad (32)$$

and $c \in \mathbb{R}_{>0}$ is a scaling parameter. For $c \rightarrow \infty$ the function \hat{P} converges towards P . Both, \hat{P} and P are depicted in Figure 5 for $c = 20$. For instance, for the former parameter choice, the maximum absolute error of α_m^* amounts to $1.13 \cdot 10^{-2}$.

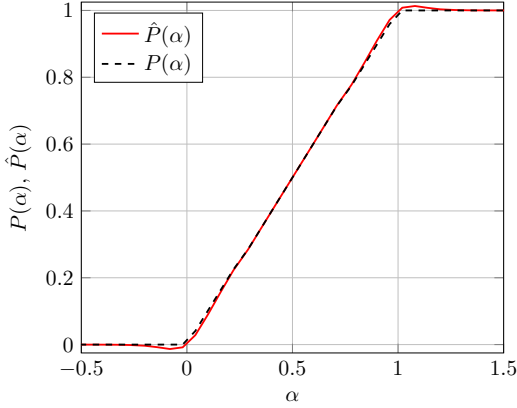


Fig. 5: A comparison between the projection operator $P(\alpha)$ and the approximated function $\hat{P}(\alpha)$ with parameter $c = 20$.

Considering the static collision avoidance, formulated in equation (16e), we follow a similar approach as explained before by approximating objects with convex bodies, i.e. by spheres or ellipsoids depending on the geometry of the considered object. In our setup, presented in Figure 1, the table represents a static object, so that there is a risk that the robot i chooses a trajectory bellow or through the table in order to avoid another robot j . For this purpose it is sufficient to formulate a plane along the table and restrict the intersection of the basis of each link \mathbf{b}_m of the robot i with the plane by the height of the table denoted as vector $\mathbf{z} = [0 \ 0 \ z_T]$, i.e.

$$\mathbf{b}_m \geq \mathbf{z} + \mathbf{z}_{\min}, \quad (33)$$

with an offset \mathbf{z}_{\min} . In case of the gripper, which is attached to the end effector, an additional offset equal to the length of the gripper should be considered.

VII. DEADLOCK

Deadlocks occurring in a setup of multiple robots is a well-known problem in the field of mobile robots, UAVs and robotic manipulators [36], [37]. The problem may arise if one or more robotic manipulators block each other, effectively preventing each other from reaching their target state. In our case, the solution of the optimization problem (16) is at a Nash equilibrium, when a deadlock occurs. Deviating from the optimal solution would increase the cost and, therefore, would not be an optimal strategy in a non-cooperative game. To this end, resolving deadlocks requires a supervisory instance, i.e. a coordinator, and some sort of information exchange between the robotic manipulators and the coordinator. Our approach regarding deadlocks, which will be presented in the following, was inspired by the work of Tallamraju et al. [37].

We introduced the role of a coordinator in Section V, that resolves the deadlock with a variable γ_i , see Figure 3. The coordinator receives the predicted state sequences $\hat{\mathbf{x}}_i^{*0:N_p}$ of each robotic manipulator and checks which robots are blocking each other. A deadlock is detected, if manipulator i does not move, i.e., the change of the predicted states is suitably small

$$\left\| \hat{\mathbf{x}}_i^{*N_p} - \hat{\mathbf{x}}_i^{*0} \right\| \leq \varepsilon \quad (34)$$

and, at the same time, the deviation of the robot's measured state \mathbf{x}_i^s and the desired state \mathbf{x}_i^f is sufficiently large

$$\left\| \mathbf{x}_i^s - \mathbf{x}_i^f \right\| \geq \delta. \quad (35)$$

The former is checked for each time step and robot by the coordinator. Should a deadlock be detected for any of the M manipulators, all manipulators which share active collision constraint with this robot are determined. Then, all manipulators of this group are deactivated except for the manipulator that is closest to its desired state. This procedure ensures, that only manipulators that are in deadlock are deactivated, whereas all other robots in the workspace are not restricted in their movement. Once the active robot overcomes the deadlock, the deactivated robots can move again.

Deadlocks in a pick and place task often occur during grasping of an object. In this case, a deadlock is resolved for other robots after a robot picked its object. For deactivation of a robot i at its current state, the cost function in (16) is extended to

$$J_i = \gamma_i \left[J_i^f(\mathbf{x}_i^{N_p}) + \sum_{k=0}^{N_p-1} J_i^c(\mathbf{x}_i^k, \mathbf{u}_i^k) \right] + (1 - \gamma_i) J_i^d(\mathbf{x}_i^k) \quad (36)$$

with an additional cost term $J_i^d(\mathbf{x}_i^k)$ and a deadlock parameter γ_i . With $\gamma_i \in \{0, 1\}$, the robot's movement to the desired state can be deactivated by setting $\gamma_i = 0$. The additional cost term $J_i^d(\mathbf{x}_i^k)$ represents a repulsive force, which acts between the robot i and neighboured robots during a deadlock, while the robot i is deactivated

$$J_i^d(\mathbf{x}_i^k) = \sum_{\substack{j=1 \\ j \neq i}}^M \max(0, d_s - \text{dist}(R_i(\mathbf{x}_i^k), R_j(\mathbf{x}_j^{*k}))^2). \quad (37)$$

Parameter d_s sets a distance from which repulsive forces are active. Once a deadlock is resolved, γ_i is set to 1 (for every involved robot) and the former deactivated robots proceed in executing their respective tasks.

VIII. RESULTS

A. Simulation setup and controller parametrization

The multi-robot setup is built in a robotic simulation environment *Gazebo* [33] with four simulated collaborative robotic manipulators UR3 from *Universal Robots*. *Gazebo* provides an interface to control the robots using the Robot Operating System (ROS) [34]. In this paper we use the distribution *ROS Melodic*. The communication is established through the ROS action client to the *Universal Robot* ROS driver. The ROS interface allows that the simulation environment *Gazebo* can easily be replaced by an experimental test bed. The four model predictive controllers run in parallel on a computer with an Intel 8700k at 3.7 GHz using 32 GB RAM under Ubuntu 16.04. The coordinator is running on the same computer and communicates the computed optimal trajectories with the controllers via the TCP/IP protocol.

The control algorithms are implemented in *Matlab* using *CasADi* [38] for setting up the non-linear program for the DMPCs. The merit of *CasADi* is its automatic differentiation capability, i.e., *CasADi* computes the first and second derivatives of the cost function and constraints using automatic differentiation. We use the interior point solver *IPOPT* [39] to solve the optimization problem and apply *MA27* [40] to solve the underlying linear system. We set the maximum number of iterations to 100 and an acceptable tolerance of 10^{-4} . In addition, *CasADi* is instructed to pre-compile the optimization problems using just-in-time compilation. We choose a sampling time of $T_s = 0.1$ s and a horizon length of $N_p = 15$, which means a prediction time of 1.5 s.

In this work we validate our motion control algorithm for a pick and place scenario comprising $M = 4$ robotic manipulators with $N = 6$ degrees of freedom each. Each robot is approximated by 8 line segments and 5 ellipsoids, resulting in 40 conceivable constraints for each pair of manipulators. That means overall 120 conceivable constraints per local DMPC. However, geometrically it is impossible to position four robots in a setup, where all constraints need to be taken into account, i.e. robots standing in a diagonal could only collide with their wrist links and robots standing next to each other will never reach the basis and shoulder links of the other one. Therefore, only 26 instead of 120 conceivable collision constraints, for each DMPC, need to be considered. Additionally, 2 static collision constraints to avoid collision with the table are taken into account.

The four robots and the objects are placed on top of a table of a height $z_T = 0.85$ m. The positions of the basis of the four

collaborative robotic manipulators in the workspace, omitting the z -coordinate, are as follows

$$\begin{aligned}\mathbf{p}_1^B &= (0.0, \quad 0.0), & \mathbf{p}_2^B &= (0.744, \quad 0.0), \\ \mathbf{p}_3^B &= (0.744, \quad 0.744), & \mathbf{p}_4^B &= (0.0, \quad 0.744).\end{aligned}$$

The four objects are placed in such a way that multiple collisions between the robots and a deadlock can occur. Therefore the positions of the objects are chosen as

$$\begin{aligned}\mathbf{O}_1 &= (0.3, \quad 0.18), & \mathbf{O}_2 &= (0.4, \quad 0.3), \\ \mathbf{O}_3 &= (1.0, \quad 0.6), & \mathbf{O}_4 &= (0.3, \quad 0.42).\end{aligned}$$

The task for each robot i is to grasp an object \mathbf{O}_i and bring it to the robot's initial configuration pose. The validation scenario consists of two consecutive tasks, which are to move to the object, grasp it and move back to the initial configuration and release the object, which are shown in Figure 8 (a,d). The initial positions of the robotic manipulators' end effectors in Cartesian space are

$$\begin{aligned}\mathbf{p}_1^0 &= (-0.4, \quad 0.2015, \quad 0.035), \\ \mathbf{p}_2^0 &= (1.2, \quad 0.2, \quad 0.035), \\ \mathbf{p}_3^0 &= (0.45, \quad 0.59, \quad 0.035), \\ \mathbf{p}_4^0 &= (-0.3, \quad 0.5184, \quad 0.035).\end{aligned}$$

The weighting matrices of the DMPCs are chosen as

$$\begin{aligned}\mathbf{Q}_i^x &= \text{diag}(1, 1, 1, 0.2, 0.2, 0.2, 1, 1, 1, 0.2, 0.2, 0.2), \\ \mathbf{Q}_i^f &= 10 \cdot \mathbf{Q}_i^x, \quad \mathbf{R}_i^u = 0.1 \cdot \mathbf{I}^{6 \times 6}, \quad \mathbf{R}_i^d = 15 \cdot \mathbf{I}^{6 \times 6}.\end{aligned}$$

Joint positions and velocities of the three wrist links are penalized less to allow for a greater freedom of motion. The joint velocities and accelerations are limited to π . The parameters for the deadlock algorithm are set as follows

$$\varepsilon = 10^{-2}, \quad \delta = 2 \cdot 10^{-2}, \quad d_s = 0.25. \quad (38)$$

B. Input delays of closed-loop non-linear model predictive control

The number of active dynamic collision constraints summarized in equation (16f) change dynamically, as not all possible collisions can occur at a time step k . The number of active collision constraints considerably affects the computation times of the non-convex optimization problem (16), which can be seen in the Table I for maximum computation times $T_{c,\max}$. Indeed, T_c might even be greater than the sampling time T_s and therefore the optimal control input u^* can not be obtained immediately.

The larger the sampling time T_s , the smaller the influence of the computation time T_c on the DMPC. However, the sampling time cannot be increased arbitrarily, otherwise tunneling will occur. For this reason, we followed the approach of Grüne and Pannek [41] to account for the non-negligible computation times. As the maximum computation time is $T_{c,\max} < 2 \cdot T_s$, we solve the DMPC every $2 \cdot T_s$, still with a sampling time T_s within the optimization.

Controller Type	$T_{c,\min}$ [ms]	$T_{c,\max}$ [ms]	$T_{c,\text{mean}}$ [ms]
Centralized MPC	120	670.5	232.9
Distributed MPC R_1	26.9	185.6	64.8
Distributed MPC R_2	22.9	128.8	38.7
Distributed MPC R_3	21.1	188.9	32.2
Distributed MPC R_4	20.1	103.3	36.1

TABLE I: Minimum, maximum and mean computation time values of distributed and centralized MPC.

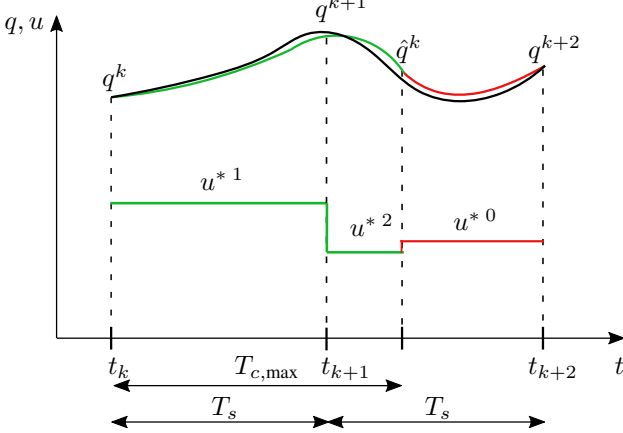


Fig. 6: Compensation of computation times $T_{c,\max} \geq T_s$ for non-linear model predictive control.

In the following, we illustrate the approach for a single joint $q \in \mathbb{R}$ and maximum computation times greater than T_s , i.e., $T_{c,\max} > T_s$ holds. At time t_k , a new measurement q^k is received from the manipulator. Due to the computation time T_c , a new optimal control input is not available at time t_k . The robot is provided the optimal control input from the last optimization step for time t_k until $t_k + T_{c,\max}$. Figure 6 illustrates this concept for $T_{c,\max} > T_s$ and the green line designates the optimal control inputs $[u^{*1} \ u^{*2}]$. Simultaneously, at time t_k , the state q^k is extrapolated into the future by integrating the manipulators dynamics $f(q(t), u(t))$

$$\hat{q}^k = q^k + \int_{t_k}^{t_k + T_{c,\max}} f(q(t), u(t)) dt. \quad (39)$$

With \hat{q}^k as the initial condition, the optimization problem (16) is solved so that a new trajectory and control input is available at the latest at time $t_k + T_{c,\max}$. At time $t_k + T_{c,\max}$ the obtained optimal control input u^{*0} , illustrated by red in Figure 6, is sent to the robot. At time event t_{k+2} the DMPC receives a new measurement q^{k+2} and the procedure is repeated. We follow Krämer et al. [21] and obtain $T_{c,\max}$ via a moving average filter over past observed delays.

C. Validation of the motion algorithm

With the compensation of input delays at hand, we turn our attention to the validation of our motion algorithm. The setup of four robots is chosen in a way to show the efficacy of the previously introduced approaches for dynamic collision avoidance and deadlock detection. Figure

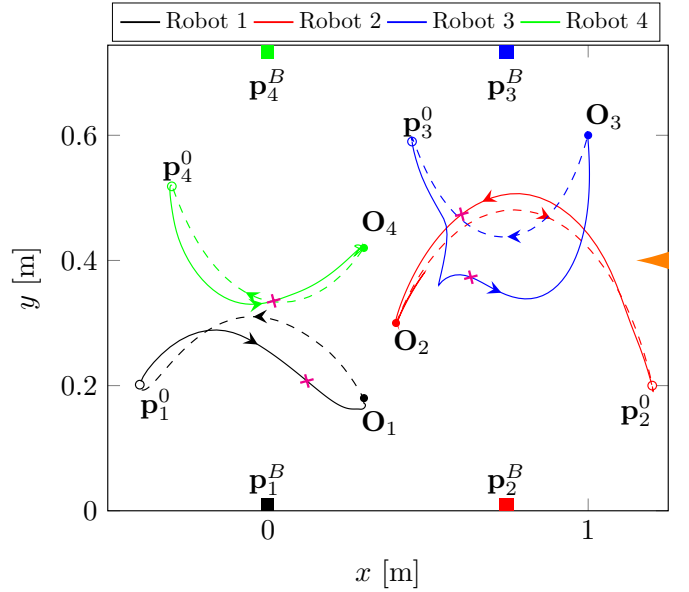


Fig. 7: Trajectory of robots' end effectors in the workspace.

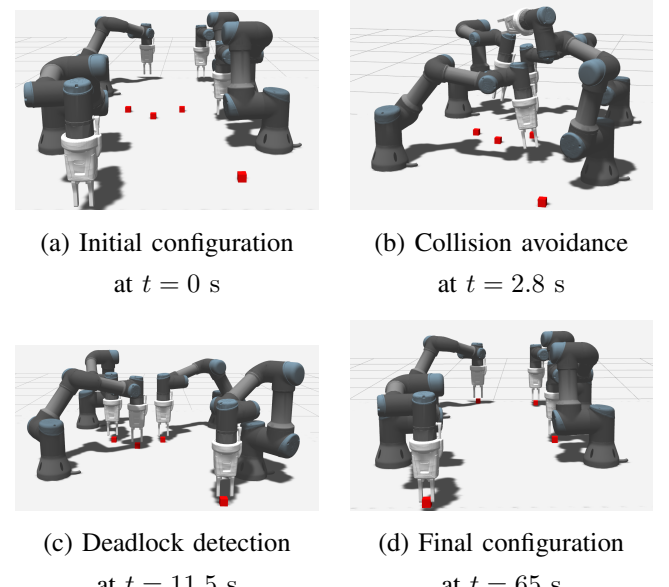


Fig. 8: Selected time frames from the simulation environment *Gazebo*.

7 shows the trajectory of the four robots' end effectors in the workspace. The robots start at positions p_1^0 for Robot 1 illustrated as black line, p_2^0 for Robot 2 illustrated as red line, p_3^0 for Robot 3 illustrated as blue line and p_4^0 for Robot 4 illustrated as green line. The arrow tip on the right border of Figure 7 indicates from which side the four robots in Figure 8 are observed. The initial and final configuration of the robots, which are identical, are shown in Figure 8a and 8d, respectively. The trajectories to the objects O_1 , O_2 , O_3 and O_4 are depicted as solid lines and the trajectories back to the final target are illustrated by dashed lines in Figure 7. The arrows indicate in which direction the robots are moving

along their trajectories.

The depicted trajectories show, that each robot chooses a different path to return to its initial position compared to the outward trajectory. Collision avoidance between the robots can be especially seen for Robot 3, whose object is placed outside the shared workspace with the robot's initial configuration inside the workspace. At time $t = 2.8$ s, Robot 3 avoids Robot 2 by moving over it. This can be observed in the 3D simulation in Figure 8b or in Figure 9 where the joint angle $q_4(t)$ of Robot 2 show noticeable deflections. This moment is indicated by crosses in the workspace trajectory in Figure 7. A closer look at Figure 10 shows that Robot 3 avoiding Robot 2 is accompanied by a slight increase of its cost function. During the same time range, Robot 1 also chooses another path in order to avoid a collision with Robot 4. A less strong deviation of the joint angle $q_4(t)$ can be seen in Figure 9.

Objects \mathbf{O}_1 , \mathbf{O}_2 and \mathbf{O}_4 are positioned in close proximity in the middle of the common workspace. Therefore, it is impossible for the manipulators 1, 2 and 4 to pick up the three objects simultaneously without causing a collision. With this case, we illustrate how the robots solve such a dilemma in a non-cooperative game, as every agent acts egoistically to achieve its own best possible benefit. Robot 1 manages to reach the target before the other robots. The other two robots 2 and 4 come in close proximity to robot 1 and prevent robot 1 from grasping the object effectively resulting in a deadlock at time $t = 11.5$ s. The former can be seen in the 3D simulation in Figure 8c. As Robot 1 is closest to its target, robots 2 and 4 are deactivated, i.e., the coordinator sets $\gamma_2 = 0$ and $\gamma_4 = 0$, until Robot 1 has grasped the object. Due to repulsive forces of the deactivated robots, Robot 1 pushes Robot 2 aside to grasp its object, which can be seen in the full line along the dashed line in Figure 7. Robot 2 is more affected as it is closer to Robot 1 and after the deadlock is resolved Robot 2 returns back to grasp its object. The cost function of Robot 1 rises at time $t = 25.6$ s, where the robot receives the next task. At the same time, the coordinator resets $\gamma_2 = 1$ and $\gamma_4 = 1$ and the deadlock is resolved. Notice, that Robot 3 executes its task unaffected by the deadlock and its resolution.

The cost function values show exactly when the robot receives a new target. High cost function values indicate that a robot received a new target and is far away from it, which can be seen in Figure 10.

In order to draw conclusions about real-time capabilities of the derived algorithm, computation times have to be considered. In Figure 11 computation times over real-time can be seen for each robot. The computation times rise significantly, when most of the collision constraints are active. This can be seen for the time range $0.1 \leq t \leq 2.7$ s highlighted in Figure 11. Further, computation times rise again at time 25.6 s, when all four robots are in the shared workspace, i.e. when Robot 3 moves to its final pose and Robot 1 grasps its object and moves to its final target. In that

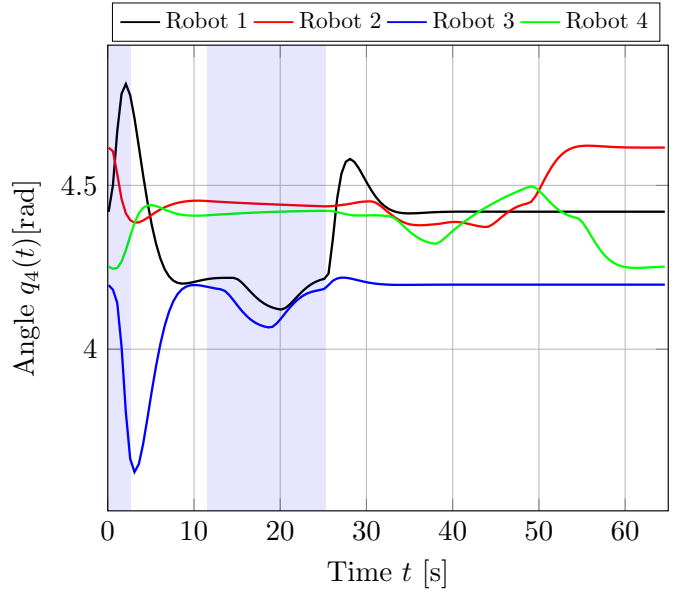


Fig. 9: First wrist position of four robotic manipulators.

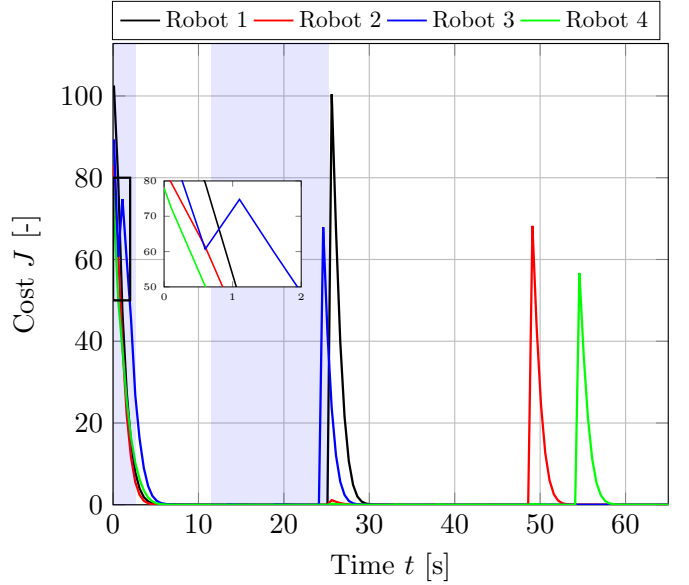


Fig. 10: Cost function of four robotic manipulators.

case, the robots have to avoid each other and the computation times of robots 1 and 2 reach another peak.

Last but not least, we discuss the computational cost and, therefore, real-time capabilities of our approach. To get an impression of the the speed-up, we compare our approach to a more traditional, centralized MPC. As the cost function J for the centralized approach, we choose the sum of the individual cost functions of the robots, i.e.

$$J = J_1 + J_2 + J_3 + J_4. \quad (40)$$

For the collision avoidance in the centralized setting, the robots are approximated with line segments and ellipsoids to ensure a comparability of the results. Table I showed

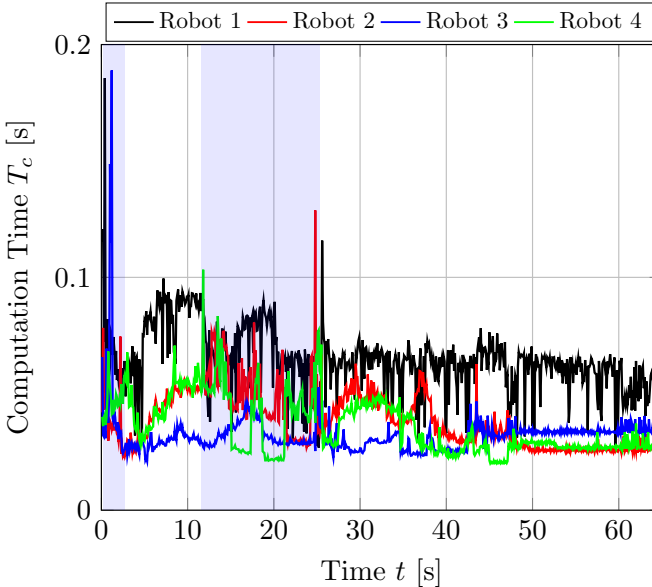


Fig. 11: Computation times for four robotic manipulators.

minimum, maximum and mean computation times for each robot. As can be seen from the table, even the minimum computation time for the centralized approach lies above the sampling time $T_s = 100$ ms. The maximum computation time is almost 7 times higher than the sampling time. Compared to the centralized MPC, minimum computation times of the distributed MPC lie considerably below the sampling time and the maximum times can be compensated by the procedure explained before. A careful comparison of computation times for centralized and distributed MPC leads to the following conclusion: A speed-up of a factor 4 can be achieved by choosing the distributed MPC over the centralized approach. This is to be expected, since the optimization problem for the centralized MPC is split into four optimization problems with one fourth of the original size. These results indicate that the distributed approach leads to real-time capable computation times which cannot be provided by the centralized MPC.

IX. CONCLUSION

In this work we introduced a novel motion control algorithm for multiple robotic manipulators. Each robot plans its own collision free trajectory accounting for static and dynamic obstacles. Our framework scales to multiple robotic manipulators allowing for a flexible operation in a shared workspace. The motion control is realized as a distributed model predictive control (DMPC), formulated as a non-cooperative game. The framework requires a communication between the manipulators. To this end, a coordinator is introduced, that shares the predicted optimal states of the robots with each other. With the received information, each robot accounts for potential collisions. We propose a novel approach to formulate the collision avoidance constraints. Each robot is approximated by line segments, while the other surrounding robots are approximated by ellipsoids. The

formulated collision constraints allow for a computation of the optimal trajectories in real-time. In a setup of multiple robotic manipulators deadlocks may occur, which is a well known problem in robotics. We derived an approach, where the introduced coordinator is able to detect and resolve deadlocks locally without interrupting the motion of not affected robots.

The motion control algorithm was validated on a setup of four robotic manipulators performing a pick and place scenario to show the scalability and real-time feasibility of the introduced approach. The setup was built in the simulation environment *Gazebo* and controlled by ROS. We observed that for intersecting trajectories, deadlocks did not occur and the robots reliably avoided each other. Deadlocks only occurred when the robots interfered with each other during grasping. However, in this case, the coordinator reliably detected and resolved the occurring deadlocks. Finally, a comparison of computation times with centralized MPC as a benchmark showed, that a speed-up of a factor of 4 is achieved by solving the problem in a distributed manner. The former indicates that our approach enables flexible, real-time capable motion control and trajectory planning of multiple robots operating in the same workspace. Due to its distributed nature, it scales easily to even more than four robotic manipulators.

In the future, we plan to realize the proposed approach on an experimental testbed for at least two robotic manipulators performing assembly and disassembly tasks. We have seen that deadlocks occur when manipulators interfere with each other during grasping an object. To further increase the efficiency of our approach, it might be beneficial to prevent deadlocks in advance by an intelligent scheduling of the tasks. Such a scheduling algorithm could be realized as a top layer of the proposed control algorithm.

REFERENCES

- [1] J. Hermann, A. David, A. Wagner, and M. Ruskowski, "Considering interdependencies for a dynamic generation of process chains for production as a service," *Procedia Manufacturing*, vol. 51, pp. 1454–1461, 2020.
- [2] M. Ruskowski, A. Herget, J. Hermann, W. Motsch, P. Pahlevannejad, A. Sidorenko, S. Bergweiler, A. David, C. Plociennik, J. Popper, K. Sivalingam, and A. Wagner, "Production Bots für Production Level 4: Skill-basierte Systeme für die Produktion der Zukunft," *atp magazin*, vol. 62, pp. 62–71, 2020.
- [3] S. Wrede, O. Beyer, C. Dreyer, M. Wojtynek, and J. Steil, "Vertical integration and service orchestration for modular production systems using business process models," *Procedia Technology*, vol. 26, pp. 259–266, 2016.
- [4] M. Kalakrishnan, S. Chitta, E. Theodorou, P. Pastor, and S. Schaal, "Stomp: Stochastic trajectory optimization for motion planning," *IEEE International Conference on Robotics and Automation*, pp. 4569–4574, 2011.
- [5] D. Verschueren, B. Demeulenaere, J. Swevers, J. De Schutter, and M. Diehl, "Time-optimal path tracking for robots: A convex optimization approach," *IEEE Transactions on Automatic Control*, vol. 54, no. 10, pp. 2318–2327, 2009.
- [6] B. Faverjon and P. Tournassoud, "A local based approach for path planning of manipulators with a high number of degrees of freedom," *IEEE International Conference on Robotics and Automation*, vol. 4, pp. 1152–1159, 1987.

[7] F. Kanehiro, F. Lamiraux, O. Kanoun, E. Yoshida, and J. P. Laumond, “A local collision avoidance method for non-strictly convex polyhedra,” *Robotics: Science and Systems*, vol. 4, no. June, pp. 151–158, 2009.

[8] C. Fang, A. Rocchi, E. M. Hoffman, N. G. Tsagarakis, and D. G. Caldwell, “Efficient self-collision avoidance based on focus of interest for humanoid robots,” *IEEE-RAS International Conference on Humanoid Robots*, pp. 1060–1066, 2015.

[9] M. Wang, J. Luo, and U. Walter, “A non-linear model predictive controller with obstacle avoidance for a space robot,” *Advances in Space Research*, vol. 57, no. 8, pp. 1737–1746, 2016.

[10] P. Bosscher and D. Hedman, “Real-time collision avoidance algorithm for robotic manipulators,” *Industrial Robot*, vol. 38, no. 2, pp. 186–197, 2011.

[11] S. M. LaValle, *Planning algorithms*. Cambridge University Press, 2006.

[12] D. Q. Mayne, J. B. Rawlings, C. V. Rao, and P. O. Scokaert, “Constrained model predictive control: Stability and optimality,” *Automatica*, vol. 36, no. 6, pp. 789–814, 2000.

[13] D. Lam, C. Manzie, and M. C. Good, “Multi-axis model predictive contouring control,” *International Journal of Control*, vol. 86, no. 8, pp. 1410–1424, 2013.

[14] M. M. G. Ardakani, B. Olofsson, A. Robertsson, and R. Johansson, “Real-time trajectory generation using model predictive control,” *IEEE International Conference on Automation Science and Engineering*, 2015.

[15] K. Belda and O. Rovny, “Predictive control of 5 DOF robot arm of autonomous mobile robotic system motion control employing mathematical model of the robot arm dynamics,” *Proceedings of the 2017 21st International Conference on Process Control, PC 2017*, pp. 339–344, 2017.

[16] M. W. Spong, S. Hutchinson, and M. Vidyasagar, *Robot modeling and control*. Wiley, 2006.

[17] C. Liu, C. Y. Lin, and M. Tomizuka, “The convex feasible set algorithm for real time optimization in motion planning,” *SIAM Journal on Control and Optimization*, vol. 56, no. 4, pp. 2712–2733, 2018.

[18] T. Schoels, P. Rutquist, L. Palmieri, A. Zanelli, K. O. Arras, and M. Diehl, “CIAO: Mpc-based safe motion planning in predictable dynamic environments,” *IFAC PapersOnLine* (in press), 2021.

[19] C. Rösmann, F. Hoffmann, and T. Bertram, “Planning of multiple robot trajectories in distinctive topologies,” pp. 1–6, 2015.

[20] J. Cascio, M. Karpenko, Q. Gong, P. Sekhavat, and I. M. Ross, “Smooth proximity computation for collision-free optimal control of multiple robotic manipulators,” *IEEE/RSJ International Conference on Intelligent Robots and Systems*, pp. 2452–2457, 2009.

[21] M. Krämer, C. Rösmann, F. Hoffmann, and T. Bertram, “Model predictive control of a collaborative manipulator considering dynamic obstacles,” *Optimal Control Applications and Methods*, vol. 41, no. 4, pp. 1211–1232, 2020.

[22] V. J. Lumelsky, “On fast computation of distance between line segments,” *Information Processing Letters*, vol. 21, no. 2, pp. 55–61, 1985.

[23] E. G. Gilbert, D. W. Johnson, and S. S. Keerthi, “A fast procedure for computing the distance between complex objects in three-dimensional space,” *IEEE Journal on Robotics and Automation*, vol. 4, no. 2, pp. 193–203, 1988.

[24] E. Rimon and S. P. Boyd, “Obstacle Collision Detection Using Best Ellipsoid Fit,” *Journal of Intelligent and Robotic Systems: Theory and Applications*, vol. 18, no. 2, pp. 105–126, 1997.

[25] C. Rösmann, M. Krämer, A. Makarow, F. Hoffmann, and T. Bertram, “Exploiting sparse structures in nonlinear model predictive control with hypergraphs,” pp. 1332–1337, 2018.

[26] M. Gerdts, R. Henrion, D. Hömberg, and C. Landry, “Path planning and collision avoidance for robots,” *Numerical Algebra, Control and Optimization*, vol. 2, no. 3, pp. 437–463, 2012.

[27] X. Zhang, A. Liniger, and F. Borrelli, “Optimization-based collision avoidance,” *IEEE Transactions on Control Systems Technology*, 2020.

[28] P. D. Christofides, R. Scattolini, D. M. de la Pena, and J. Liu, “Distributed model predictive control: A tutorial review and future research directions,” *Computers & Chemical Engineering*, vol. 51, pp. 21–41, 2013.

[29] M. Flad, L. Fröhlich, and S. Hohmann, “Cooperative shared control driver assistance systems based on motion primitives and differential games,” *IEEE Transactions on Human-Machine Systems*, vol. 47, no. 5, pp. 711–722, 2017.

[30] Y. He, M. Wu, and S. Liu, “An optimisation-based distributed cooperative control for multi-robot manipulation with obstacle avoidance,” *IFAC PapersOnLine* (in press), 2021.

[31] A. Tika, N. Gafur, V. Yfantis, and N. Bajcinca, “Optimal scheduling and model predictive control for trajectory planning of cooperative robot manipulators,” *IFAC PapersOnLine* (in press), 2021.

[32] A. Tika and N. Bajcinca, “Synchronous minimum-time cooperative manipulation using distributed model predictive control,” *2020 IEEE/RSJ International Conference on Intelligent Robots and Systems*, 2020.

[33] N. Koenig and A. Howard, “Design and use paradigms for gazebo, an open-source multi-robot simulator,” *IEEE/RSJ International Conference on Intelligent Robots and Systems*, vol. 3, pp. 2149–2154, 2004.

[34] Stanford Artificial Intelligence Laboratory et al., “Robotic operating system.” [Online]. Available: <https://www.ros.org>

[35] B. T. Stewart, A. N. Venkat, J. B. Rawlings, S. J. Wright, and G. Pannocchia, “Cooperative distributed model predictive control,” *Systems & Control Letters*, vol. 59, no. 8, pp. 460–469, 2010.

[36] M. Jager and B. Nebel, “Decentralized collision avoidance, deadlock detection, and deadlock resolution for multiple mobile robots,” *IEEE/RSJ International Conference on Intelligent Robots and Systems*, pp. 1213–1219, 2001.

[37] R. Tallamraju, S. Rajappa, M. J. Black, K. Karlapalem, and A. Ahmad, “Decentralized mpc based obstacle avoidance for multi-robot target tracking scenarios,” *IEEE International Symposium on Safety, Security, and Rescue Robotics*, pp. 1–8, 2018.

[38] J. A. E. Andersson, J. Gillis, G. Horn, J. B. Rawlings, and M. Diehl, “CasADi – A software framework for nonlinear optimization and optimal control,” *Mathematical Programming Computation*, vol. 11, no. 1, pp. 1–36, 2019.

[39] A. Wächter and L. T. Biegler, “On the implementation of an interior-point filter line-search algorithm for large-scale nonlinear programming,” *Mathematical programming*, vol. 106, no. 1, pp. 25–57, 2006.

[40] H. S. Library, “A collection of fortran codes for large-scale scientific computation,” <http://www.hsl.rl.ac.uk>, 2018.

[41] L. Grüne and J. Pannek, *Nonlinear model predictive control*. Springer, 2017.